

# Passively mode-locked grown-together composite YVO<sub>4</sub>/Nd:YVO<sub>4</sub> crystal laser with a semiconductor saturable absorber mirror under 880-nm direct pumping

Fangqin Li (李芳琴)<sup>1,2,3</sup>, Nan Zong (宗楠)<sup>1</sup>, Zhichao Wang (王志超)<sup>1,3</sup>, Lin Han (韩琳)<sup>1</sup>, Yong Bo (薄勇)<sup>1</sup>, Qinjun Peng (彭钦军)<sup>1\*</sup>, Dafu Cui (崔大复)<sup>1</sup>, and Zuyan Xu (许祖彦)<sup>1</sup>

<sup>1</sup>Research Center of Laser Physics and Technology, Key Laboratory of Functional Crystal and Technology, Technical Institute of Physics and Chemistry, Chinese Academy of Sciences, Beijing 100190, China

<sup>2</sup>Key Laboratory of Optical Physics, Institute of Physics, Chinese Academy of Sciences, Beijing 100190, China

<sup>3</sup>Graduate University of the Chinese Academy of Sciences, Beijing 100049, China

\*Corresponding author: pengqinjun@163.com

Received October 22, 2010; accepted December 14, 2010; posted online March 14, 2011

A passively mode-locked grown-together composite YVO<sub>4</sub>/Nd:YVO<sub>4</sub> crystal laser is demonstrated with a semiconductor saturable absorber mirror by 880-nm laser-diode direct pumping. Under the absorbed pump power of 24.9 W, a maximum output power of 10.5 W at the repetition rate of 77 MHz is obtained, corresponding to the optical-optical conversion efficiency of 42.1% and the slope efficiency of 53.4%. The pulse width measured is 33 ps at the output power of 10 W.

OCIS codes: 140.3480, 140.3580, 140.4050, 160.3380.

doi: 10.3788/COL201109.041405.

Compact passively mode-locked laser diode (LD) pumped solid-state lasers with semiconductor saturable absorber mirrors (SESAMs) have been attractive for various applications, such as precision micromachining and nonlinear frequency conversion. The neodymium-doped vanadate Nd:YVO<sub>4</sub> crystal has been extensively used for LD pumped passively mode-locked lasers because of its high absorption coefficient for diode pumping and large stimulated emission cross section<sup>[1–5]</sup>. However, because of the weak thermal conductivity of Nd:YVO<sub>4</sub> crystal, its application in high-power mode-locked laser system is limited. In recent years, many investigations have focused on LD direct pumping at 879 and 880 nm<sup>[6–8]</sup> or have used composite YVO<sub>4</sub>/Nd:YVO<sub>4</sub> crystals<sup>[8–10]</sup> to reduce the thermal effects. The LD direct pumping reduces the quantum defect due to the closer match between the pump and the laser wavelengths compared with the traditional 808-nm pumping. By using 880-nm pumping, an average output power of 4.76 W is generated from a continuous-wave (CW) mode-locked Nd:YVO<sub>4</sub> laser<sup>[11]</sup>. In the composite YVO<sub>4</sub>/Nd:YVO<sub>4</sub> crystal, the undoped YVO<sub>4</sub> section serves as a heat sink for the pumping surface to reduce the thermal load. Composite YVO<sub>4</sub>/Nd:YVO<sub>4</sub> crystals can be obtained either by diffusion bonding method or continuous-grown technique<sup>[12]</sup>. Using a diffusion-bonding composite YVO<sub>4</sub>/Nd:YVO<sub>4</sub> crystal, the mode-locked power of 10.15 W has been reported under 808-nm LD pumping<sup>[13]</sup>. Currently, based on continuous-grown or grown-together composite YVO<sub>4</sub>/Nd:YVO<sub>4</sub> crystals, only CW and Q-switched lasers have been reported under direct pumping<sup>[8]</sup>.

In this letter, we report a passively mode-locked grown-together composite YVO<sub>4</sub>/Nd:YVO<sub>4</sub> crystal laser at 1064 nm with a SESAM under 880-nm LD direct pumping. An average mode-locked power of 10.5 W at a repetition rate of 77 MHz is obtained under the absorbed pump

power of 24.9 W, corresponding to the optical-optical conversion efficiency of 42.1% and the slope efficiency of 53.4%. The pulse width is measured to be 33 ps at the output power of 10 W. Due to the reduced thermal lens effect caused by the use of the grown-together composite crystal as well as the direct pumping scheme, no saturation of the output power is observed, and higher mode-locked power can be obtained if the laser cavity will be further optimized when increasing the pump power. During the experiment, no Q-switching mode locking (QML) but rather multiple-pulse states are observed before CW mode locking is achieved. This phenomenon can be attributed to the large third-order nonlinearity of the composite YVO<sub>4</sub>/Nd:YVO<sub>4</sub> crystal.

Figure 1 shows the scheme of the experimental setup. An a-cut grown-together composite YVO<sub>4</sub>/Nd:YVO<sub>4</sub> crystal was used as the laser gain medium. The total dimension of the laser crystal was 3 mm in diameter and 31 mm in length, consisting of 5-mm undoped YVO<sub>4</sub> end cap and a 26-mm-long 0.7 at.-% Nd-doped section. Both end surfaces of the composite YVO<sub>4</sub>/Nd:YVO<sub>4</sub> crystal was antireflection coating at 1064 and 885 nm, and the undoped end cap was wedged 0.5° to suppress the potential Fabry-Perot etalon effect. To remove the generated heat, the laser rod was equipped in a water-cooling system with water temperature of 19 °C. An 885-nm fiber-coupled LD was used as the pump source. The core diameter and numerical aperture (NA) of the fiber were 400 μm and 0.22, respectively. As the center emitting wavelength of the LD varied with its working current and temperature, the LD was cooled at the temperature of 26 °C to meet the absorption peak of the Nd:YVO<sub>4</sub> crystal around 880 nm; the absorbance of the pump was more than 95% in our experiment. The pump radiation from the fiber was reimaged into the laser crystal by some coupling lenses, resulting in a radius of ~450 μm at the center of the crystal. The laser

cavity was a folded resonator with four mirrors and a SESAM. The input and folding mirror M2 was a plane mirror with antireflection coating at 885 nm and high-reflectance coating at 1064 nm. The folding mirrors M3 and M4 with high-reflectance coating at 1064 nm were concave mirrors with the curvature radii of 100 and 70 cm, respectively. A flat wedged mirror M1 with 20% transmission at 1064 nm was used as the output coupler. M2 and M3 were separated by about 75 cm, and the distance between M3 and M4 was about 78 cm. The SESAM was placed about 33 cm away from M4. The saturation fluence, modulation depth, and absorption recovery time of the SESAM were about  $60 \mu\text{J}/\text{cm}^2$ , 1.0%, and  $\sim 20$  ps, respectively. The SESAM was attached to a water-cooled copper heat sink with water temperature of  $19^\circ\text{C}$ . The total cavity length was about 190 cm. Using the  $ABCD$  matrix formalism, the laser mode radii were calculated to be approximately  $394\text{--}411 \mu\text{m}$  in the composite crystal and  $185\text{--}225 \mu\text{m}$  on the SESAM, with varying pump power.

The leakage radiation from M3 was detected by an ultrafast InGaAs photodetector with rise time of  $<40$  ps (UPD-40-UVIR-P, ALPHALAS GMBH, Germany), which was connected to a digital oscilloscope bandwidth of 8 GHz (DSO 80804B, Agilent, USA) throughout the experiment.

Initially, the CW performance was studied for the 880-nm LD pumped grown-together composite  $\text{YVO}_4/\text{Nd}:\text{YVO}_4$  crystal laser. In this investigation, the SESAM was replaced by a plane mirror with high-reflectance coating at 1064 nm. Figure 2 shows the average output power as a function of the absorbed pump power in CW operation and CW mode-locked operation. In the CW operation, the laser began to oscillate at the absorbed pump power of 3.3 W. At an absorbed pump power of 36.9 W, 19-W output power was obtained with a slope efficiency ( $\eta_s$ ) of 59.4% and an optical-optical efficiency ( $\eta_o$ ) of 51.5%. No roll off was observed, but we did not increase the pump power further for the safety of the crystal. In the CW mode-locked operation, the laser threshold ( $P_{\text{th}}$ ) increased to 5.6 W; at the absorbed pump power of 24.9 W, a mode-locked power of 10.5 W was obtained corresponding to the slope efficiency of 53.4% and the optical-optical efficiency of 42.1%. The pump was not increased here further due to the deterioration of the laser beam quality that disturbs the mode-locked pulses; the lower efficiency than that of the CW operation was attributed to the greater cavity loss introduced by the SESAM. Note that although a comparable 10.15-W mode-locked power with 43.2% optical-optical efficiency is reported based on a diffusion-bonding composite

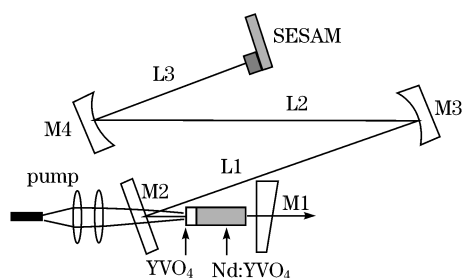


Fig. 1. Scheme of the experimental setup.

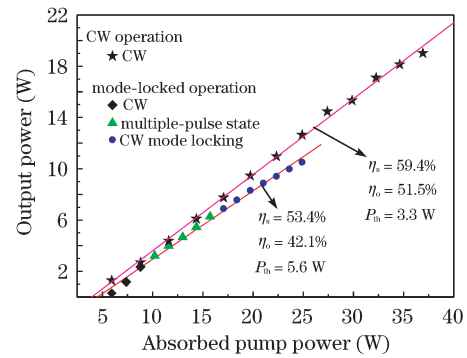


Fig. 2. Average output power as a function of the absorbed pump power in CW operation and mode-locked operation.

$\text{YVO}_4/\text{Nd}:\text{YVO}_4$  crystal under 808-nm LD pumping, the optical-optical efficiency of 45% for the CW operation is lower than ours, and their mode-locked power is difficult to scale further due to the saturation of the output power caused by thermal effects<sup>[13]</sup>.

In our case, no roll off of the output power was observed due to the 880-nm LD direct pumping that reduced thermal loading in the laser crystal. As indicated from the CW operation of the laser, the deterioration of the laser beam quality for the CW mode-locked operation was mainly caused by mode mismatching between the laser and pump modes instead of the thermal effects when the absorbed pump power was greater than 24.9 W. Thus, if the cavity was further optimized to meet the good matching between the laser and pump modes in the laser medium at higher pump power, more CW mode-locked output power would be achieved; this would be further studied in our following work. Before CW mode locking was achieved, the mode-locked laser exhibited multiple-pulse states instead of the QML regime, which was often observed and harmful to the SESAM in a SESAM-based passively mode-locked laser. Studies have shown that  $\text{YVO}_4$  crystals have a considerable value of the third-order susceptibility<sup>[14]</sup>. Based on the large third-order nonlinearity, self-starting Kerr-lens mode-locked Nd:YVO<sub>4</sub> lasers have been demonstrated experimentally, with the laser output exhibiting spontaneous mode locking<sup>[15]</sup>. Thus, the suppression of the QML and the presence of the multiple-pulse operation in our experiment may also be attributed to the third-order nonlinearity of the laser medium. The multiple-pulse states at the absorbed pump power of 11.6 and 15.5 W are illustrated in Figs. 3(a) and (b), respectively. With the increase in pump power, weak pulses were suppressed and the CW background decreased as the laser intensity on the SESAM became stronger. When the absorbed pump power was slightly higher than 16 W, CW mode locking was achieved, with the laser output power at 6.4 W. At the absorbed pump power of 18.4–24.9 W, stable CW mode locking of the laser system was observed, corresponding to the output power of 7.6–10.5 W. The stable CW mode-locking pulse trains on two different time scales are shown in Figs. 3 (c) and (d). Figure 3 (c) shows the pulse trains with time resolution of 20 ns/div, demonstrating the mode-locked pulses. The repetition rate was about 77 MHz, matching the optical cavity length. Figure 3 (d) shows the pulse trains with time resolution of 10  $\mu\text{s}/\text{div}$ , demonstrating

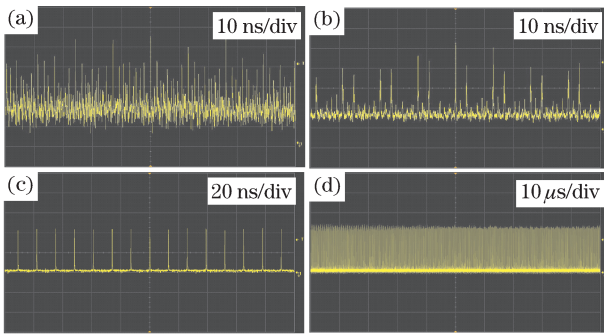


Fig. 3. Pulse trains for multiple-pulse states before CW mode locking at the absorbed pump power of (a) 11.6 and (b) 15.5 W with time resolution of 10 ns/div. Pulse trains for stable mode locking with time resolution of (c) 20 ns/div, demonstrating the mode-locked pulses, and (d) 10  $\mu$ s/div, demonstrating the amplitude stability.

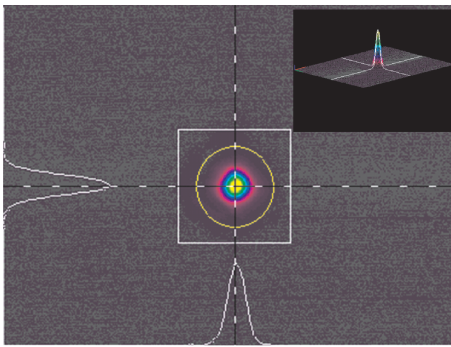


Fig. 4. Two- and three-dimensional laser beam profiles at the output power of 10.0 W.

amplitude stability.

Although no QML operation was observed during the experiment, the critical pulse energy for CW mode locking could still be predicted by the theory of  $Q$ -switching stability limits of CW passive mode locking<sup>[16]</sup>. The critical pulse energy  $E_{P,c}$  for CW mode locking based on SESAM can be estimated by<sup>[16]</sup>

$$E_{P,c} = \sqrt{F_{\text{sat,L}} A_{\text{sat,L}} F_{\text{sat,A}} A_{\text{sat,A}} \Delta R}, \quad (1)$$

where  $F_{\text{sat,L}} = h\nu/m\sigma_L$  denotes the saturation fluence of the gain medium with the Planck constant  $h$ , the laser frequency  $\nu$ , the stimulated emission cross section  $\sigma_L$ , and the number of passes through the gain medium per cavity round trip  $m$ ;  $F_{\text{sat,A}}$  denotes the saturation fluence of the absorber;  $A_{\text{sat,L}}$  and  $A_{\text{sat,A}}$  are the effective laser mode areas inside the gain medium and on the absorber, respectively;  $\Delta R$  is the modulation depth of the absorber. The saturation fluence of Nd:YVO<sub>4</sub> is estimated to be 37 mJ/cm<sup>2</sup>.  $A_{\text{sat,L}} = \pi\omega_L^2$  and  $A_{\text{sat,A}} = \pi\omega_A^2$  are estimated by the laser mode radii  $\omega_L$  in the laser crystal and  $\omega_A$  on the SESAM, respectively. For a standing-wave cavity,  $m = 2$ . Therefore, the critical pulse energy for CW mode locking is estimated to be around 411 nJ. The experimental critical pulse energy for CW mode locking was about 416 nJ, which agreed with the theoretical prediction.

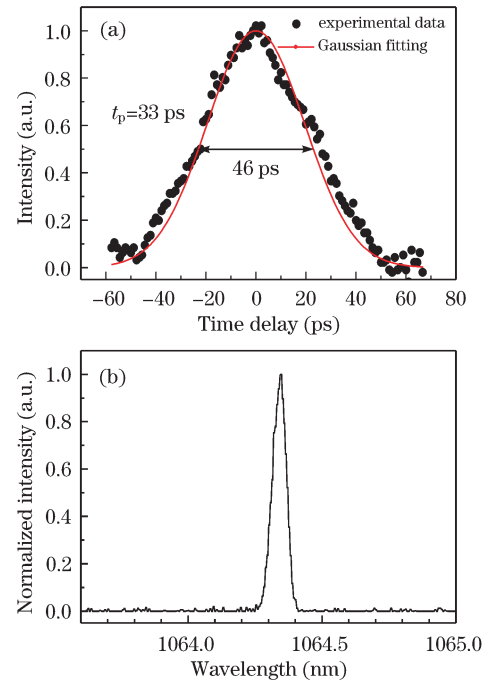


Fig. 5. (a) Autocorrelation trace of the mode-locked laser at output power of 10.0 W. Gaussian shape was assumed to determine the pulse width; (b) optical spectrum of the mode-locked laser at output power of 10.0 W.

The laser beam quality was measured with a laser beam analyzer ( $M^2$ -200, Spiricon, USA) when the laser system operated in the stable CW mode locking. The two- and three-dimensional laser beam profiles at the output power of 10.0 W are shown in Fig. 4. The beam-propagation factor  $M^2$  was measured to be 1.3, 1.4, 1.5 and 1.5 at the output power of 8.3, 9.4, 10.0, and 10.5 W, respectively. Thus, the TEM<sub>00</sub> mode ( $M^2 \leq 1.5$ ) operation is obtained through the stable CW mode locking.

The laser pulse width was measured with a home-made autocorrelator. Figure 5(a) shows the normalized intensity autocorrelation trace of the mode locked 1064-nm laser at the output power of 10.0 W. Fitting the experimental data by a Gaussian function, the pulse width of the 1064-nm laser was estimated to be 33 ps. The optical spectrum was also measured by an optical spectrum analyzer (MS9710B, Anritsu) as shown in Fig. 5(b). The spectrum width was about 0.066 nm at the center frequency of 1064.35 nm. The time-bandwidth product was calculated to be about 0.576, indicating that the output beam was a chirped pulse. The narrow spectrum width here can have arisen from the residual etalon effect of the laser crystal.

In conclusion, we have successfully demonstrated a passively mode-locked grown-together composite YVO<sub>4</sub>/Nd:YVO<sub>4</sub> crystal laser at 1064 nm with a SESAM using 880-nm diode direct pumping. Under the absorbed pump power of 24.9 W, an average output power of 10.5 W is obtained at the repetition rate of 77 MHz, corresponding to the optical-optical conversion efficiency of 42.1% and the slope efficiency of 53.4%. The pulse width is measured to be about 33 ps at the output power of 10 W, and TEM<sub>00</sub>-mode operation is observed during the stable mode locking. The experimental result reveals that the combination of a grown-together compos-

ite YVO<sub>4</sub>/Nd:YVO<sub>4</sub> crystal and the LD direct pumping scheme is beneficial to high-power, high-efficiency passively mode-locked lasers with a SESAM.

This work was supported by the National “973” Project of China under Grant No. 2010CB630706.

## References

1. A. Agnesi, C. Pennacchio, G. C. Reali, and V. Kubecek, *Opt. Lett.* **22**, 1645 (1997).
2. D. Burns, M. Hetterich, A. I. Ferguson, E. Bente, M. D. Dawson, J. I. Davies, and S. W. Bland, *J. Opt. Soc. Am. B* **17**, 919 (2000).
3. J. Y. Peng, J. G. Miao, Y. G. Wang, B. S. Wang, H. M. Tan, L. S. Qian, and X. Y. Ma, *Opt. Laser Technol.* **39**, 1135 (2007).
4. W. Wang, J. Liu, F. Chen, L. Li, and Y. Wang, *Chin. Opt. Lett.* **7**, 706 (2009).
5. X. Wushouer, H. Yu, P. Yan, and M. Gong, *Chin. Opt. Lett.* **8**, 1004 (2010).
6. Y. Sato, T. Taira, N. Pavel, and V. Lupei, *Appl. Phys. Lett.* **82**, 844 (2003).
7. P. Zhu, D. Li, P. Hu, A. Schell, P. Shi, C. R. Haas, N. Wu, and K. Du, *Opt. Lett.* **33**, 1930 (2008).
8. X. Li, X. Yu, F. Chen, R. Yan, J. Yu, and D. Chen, *Opt. Express* **17**, 12869 (2009).
9. M. Tsunekane, N. Taguchi, and H. Inaba, *Electron. Lett.* **32**, 40 (1996).
10. Z. Zhuo, T. Li, X. Li, and H. Yang, *Opt. Commun.* **274**, 176 (2007).
11. L. Sun, L. Zhang, H. J. Yu, L. Guo, J. L. Ma, J. Zhang, W. Hou, X. C. Lin, and J. M. Li, *Laser Phys. Lett.* **7**, 711 (2010).
12. J. Goujon and O. Musset, in *Proceedings of Advanced Solid-State Photonics, Technical Digest (OSA) WB5* (2008).
13. Z. Zhuo, T. Li, and Y. G. Wang, *Laser Phys. Lett.* **5**, 421 (2008).
14. A. A. Kaminskii, K. Ueda, H. J. Eichler, Y. Kuwano, H. Kouta, S. N. Bagaev, T. H. Chyba, J. C. Barnes, G. M. A. Gad, T. Murai, and J. Lu, *Opt. Commun.* **194**, 201 (2001).
15. H. C. Liang, Ross C. C. Chen, Y. J. Huang, K. W. Su, and Y. F. Chen, *Opt. Express* **16**, 21149 (2008).
16. C. Hönninger, R. Paschotta, F. Morier-Genoud, M. Moser, and U. Keller, *J. Opt. Soc. Am. B* **16**, 46 (1999).